



Sclerosing Paragangliomas: Correlations of Histological Features with Patients' Genotype and Vesicular Monoamine Transporter Expression

Angela Pucci¹ · Alessandra Bacca² · Ivana Barravecchia³ · Iosè Di Stefano¹ · Beatrice Belgio¹ · Daniele Lorenzini^{1,8} · Liborio Torregrossa¹ · Serena Chiacchio⁴ · Caterina Congregati⁵ · Gabriele Materazzi⁶ · Mauro Ferrari⁷ · Debora Angeloni³ · Giampaolo Bernini² · Fulvio Basolo¹

Received: 29 December 2021 / Accepted: 13 April 2022 / Published online: 7 May 2022
© The Author(s), under exclusive licence to Springer Science+Business Media, LLC, part of Springer Nature 2022

Abstract

Paragangliomas and pheochromocytomas are rare neuroendocrine tumors, carrying a germ-line mutation in 40% patients. Sclerosis is a rare histological feature in these tumors. We investigated the possible correlations between histological findings, first sclerosis, immunoreactivity for vesicular catecholamine transporters (VMAT1/VMAT2) and patients' genotype in a consecutive series of 57 tumors (30 paragangliomas and 27 pheochromocytomas) from 55 patients. The M-GAPP grading system, sclerosis (0–3 scale) and VMAT1/VMAT2 (0–6 scale) immunoreactivity scores were assessed. Germ-line mutations of Succinate Dehydrogenase genes, RET proto-oncogene and Von Hippel Lindau tumor suppressor gene were searched. A germ-line mutation was found in 25/55 (45.5%) patients, mainly with paraganglioma (N = 14/30, 46,66%). Significant (score ≥ 2) tumor sclerosis was found in 9 (16.1%) tumors, i.e., 7 paragangliomas and 2 pheochromocytomas, most of them (8/9) from patients with a germ-line mutation. M-GAPP score was higher in the mutation status (in 76% of patients involving the *SDHx* genes, in 12% the RET gene and in the remaining 12% the VHL gene) and in tumors with sclerosis ($p < 0.05$). Spearman's rank correlation showed a strong correlation of germ-line mutations with M-GAPP ($p < 0.0001$) and sclerosis ($p = 0.0027$) scores; a significant correlation was also found between sclerosis and M-GAPP scores ($p = 0.029$). VMAT1 expression was higher in paragangliomas than in pheochromocytomas ($p = 0.0006$), the highest scores being more frequent in mutation-bearing patients' tumors ($p < 0.01$). VMAT2 was highly expressed in all but two negative tumors. Sclerosis and VMAT1 expression were higher in paragangliomas than in pheochromocytomas; tumor sclerosis, M-GAPP and VMAT1 scores were associated to germ-line mutations. Sclerosis might represent a histological marker of tumor susceptibility, prompting to genetic investigations in paragangliomas.

Keywords Paragangliomas · Pheochromocytomas · Sclerosis · Germ-line mutation · Genotype · Vesicular monoamine transport proteins · Immunohistochemistry

✉ Angela Pucci
angelapucci@libero.it

¹ Department of Histopathology, Pisa University Hospital and Pisa University (FB), Via Roma, 57, 56126 Pisa, Italy

² Department of Clinical and Experimental Medicine, Pisa University Hospital and Pisa University (FB), Pisa, Italy

³ Institute of Life Sciences, Scuola Superiore Sant'Anna, Pisa, Italy

⁴ Department of Diagnostic, Interventional and Vascular Radiology and of Nuclear Medicine, Pisa University Hospital and Pisa University, Pisa, Italy

⁵ Department of Translational Research and New Medical Technology, Pisa University Hospital and Pisa University, Pisa, Italy

⁶ Department of Surgical, Molecular and Clinical Pathology and Critical Care, Pisa University Hospital and Pisa University, Pisa, Italy

⁷ Department of Cardiovascular Surgery, Pisa University Hospital and Pisa University, Pisa, Italy

⁸ Present Address: INT (National Institute of Tumors), Milan, Italy

Introduction

Pheochromocytomas (PHEOs) and paragangliomas (PGs) are rare (0.6 cases per 100,000 person-years) and histologically similar neuroendocrine tumors with adrenal or extra-adrenal localization, respectively [1]. The adrenal tumors may be incidentally diagnosed by imaging, whereas head-and-neck PGs (HNPGs) usually manifest as painless and slowly growing masses, catecholamine hyper-secretion rarely occurring in the latter ones. Their diagnosis is still difficult, although biochemical testing and imaging investigations have improved the diagnostic chances [1, 2]. About 40% of the affected patients carry a germ-line mutation and genetic tests may help in diagnosing familial and asymptomatic cases [1, 2]. Germ-line mutations associated with PHEO or PG have been identified in at least 19 susceptibility genes, the specific gene mutation reflecting the clinical phenotype and influencing the clinical management strategies [1–5]. Hereditary HNPGs have been linked to mutations in genes encoding one of different subunits of the succinate dehydrogenase (SDH) enzyme complex [3–7]. Susceptibility to PHEO and PG is an established component of five genetic syndromes, i.e., type 2 A (MEN2A), 2B (MEN2B) or 5 (MEN5) Multiple Endocrine Neoplasias, type 1 Neurofibromatosis (NF1), von Hippel Lindau Syndrome (VHL), and Carney-Stratakis Dyad [8, 9]. In many patients with syndromic or sporadic mutations, the clinical phenotype is often characterized by multiple, metachronous or synchronous tumours [8, 9]. The genes most frequently associated with multiple PGs are SDHAF2 (75%), SDHD (66%), RET (66%), FH (60%), VHL (40–60%), EPAS1 (50%) and MAX (50%) whereas the genes most frequently implicated in the pathogenesis of bilateral PHEOs are RET (66%), TMEM127 (15–66%), VHL (40–60%), MAX (50%) and NF1 (20–40%) [9]. Germ-line mutations in the VHL gene and in the SDHD gene have also been found in 15–20% of PHEOs with non-familial presentations [1].

Most PGs and PHEOs show a zellballen (alveolar) pattern, consisting of nests of polygonal tumor cells. Other patterns have been described; in particular, a pseudo-rosette pattern has been considered suggestive of SDHB mutated tumors [10]. Sclerosis is a rare histologic feature of these neuroendocrine tumors [11, 12]. In sclerosing tumors, the neoplastic cells are embedded in a fibrous stroma and may show cytological atypia mimicking a desmoplastic and infiltrating malignant neoplasia [13, 14].

The biological behaviour of PHEOs and PGs is unpredictable [1, 3]. The predictive value of tumor size, proliferation index and cyto-architectural features is controversial [10, 15]. Several grading systems, mainly based on histological and biological parameters (i.e., vascular invasion, secretory activity, specific growth patterns, necrosis type, proliferation

index and genetic status) have been proposed for the prediction of metastatic potential, but they have not demonstrated satisfactory sensitivity and specificity, so far [15].

The chromaffin cells of adrenal medulla and extra-adrenal paraganglia are characterized by a vesicular monoamine transporter (VMAT) system, including VMAT1 and VMAT2 that are responsible for the uptake and vesicular storage of catecholamines [16, 17]. We have recently shown that VMAT1 and VMAT2 expression is apparently independent from 18 F-DOPA PET/TC and 123-I-MIBG uptake in PGs and PHEOs [17].

The aim of the present study was to investigate the possible relationships between histological features (including tumor sclerosis), patients' genotype and VMAT1/VMAT2 tumor expression in a consecutive series (N = 57) of PGs and PHEOs from a single Center.

Materials and Methods

Study Population

Fifty-seven consecutive tumors from 55 patients with clinical diagnosis of PHEO or PG entered this retrospective study (Table 1). Patients' population included 36 F and 19 M with a mean age of 45.8 (range 14–74) years. Signs and/or symptoms of catecholamine excess were seen in 52.7% (29/55) patients, mass-related symptoms were present in 38.2% (21/55) and 5 patients were asymptomatic at presentation. Measurement of 24-hour urinary metanephrines and normetanephrines by radioimmunoassay (RIA) method was performed in all but 4 patients that lacked 24-hour urinary excretion data (Immuno Biological Laboratories, Hamburg, Germany). Normal values (n.v.) for normetanephrines were considered < 600 µg/24 hrs and for metanephrines < 350 µg/24 hrs. Tumors from patients without symptoms of catecholamine excess and/or increased normetanephrines or metanephrines levels were considered non-functioning tumors [3]. Forty-two patients underwent computed tomography (CT) and 38 magnetic resonance (MR); in a subset of patients, 123-I-MIBG scintigraphy (N = 20) or 18 F-DOPA PET/TC (N = 14) were performed and other 3 patients underwent both procedures [17, 18].

No patient underwent tumor biopsy or ablation procedure before surgical excision of the mass. The study was approved by the Ethical Committee and conformed to the Declaration of Helsinki; the informed consent was obtained from each patient.

Histology and Immunohistochemistry

All the specimens, constituted by resected tumors, were formalin-fixed and paraffin-embedded (FFPE), routinely stained

Table 1 Tumor diagnosis in 55 consecutive patients

Patient N.	Sex	Age	Diagnosis
1	F	16	HNPG
2	F	51	HNPG
3	M	52	HNPG
4	F	38	HNPG
5	F	27	HNPG
6	M	36	HNPG
6	M	37	Bronchial PG
7	M	16	HNPG
8	F	19	HNPG
9	F	56	HNPG
10	M	39	HNPG
11	F	56	HNPG
12	F	46	PHEO
13	F	14	PHEO
14	F	42	Bilateral PHEO
15	F	69	PHEO
16	M	38	PHEO
17	M	58	PHEO
18	F	35	Bilateral PHEO
19	F	27	PHEO + APG
20	F	37	PHEO
21	M	45	PHEO
22	M	69	APG
23	F	54	APG
24	M	28	APG
25	F	18	PHEO (Metastatic)
26	F	63	HNPG
27	F	48	HNPG
28	F	45	HNPG
29	F	54	HNPG
30	F	45	HNPG
31	F	64	HNPG
32	F	40	HNPG
33	F	55	HNPG
34	M	46	HNPG
35	F	69	HNPG
36	M	37	HNPG + APG + CTPG
37	F	35	PHEO
38	F	57	PHEO
39	F	48	PHEO
40	F	74	PHEO
41	F	50	PHEO
42	F	45	PHEO (Metastatic)
43	F	74	PHEO
44	M	29	PHEO
45	F	44	PHEO
46	F	58	PHEO
47	M	36	PHEO
48	F	43	PHEO
49	F	58	PHEO

Table 1 (continued)

Patient N.	Sex	Age	Diagnosis
50	M	56	PHEO
51	M	73	APG
52	M	50	Functioning APG
53	M	47	Multiple APG
54	M	35	Functioning APG (Metastatic)
55	M	55	PHEO (Metastatic)
55	M	57	PHEO (Metastasis)

HNPG head & neck paraganglioma; *PHEO* pheochromocytoma; *APG* abdominal paraganglioma; *CTPG* cervico-thoracic paraganglioma

by haematoxylin and eosin technique and classified according to the WHO Classification criteria [10]. Tumors with ≤ 5 cm maximum diameter were entirely paraffin-embedded and histologically analyzed, whereas tumors > 5 cm were sampled in a way that at least half of the tumor was submitted for histological examination. The modified grading system for adrenal PHEO and PG (M-GAPP) was performed in 52/57 (91.2%) tumors from 51 patients: the remaining 4 patients (N. 5, 15, 31, 44; Table 2) lacked diuresis data for catecholamine evaluation and the 5th tumor was a lymph node metastasis (patient n. 55; Table 2) [19–21]. For this study, the genetic evaluation of SDHx mutations replaced the non-available SDHB immunostaining in the M-GAPP score [22, 23]. The extent of sclerosis was evaluated on the whole central section of the tumor. The presence of intra-tumor sclerosis, namely the deposition of collagenous stroma between tumor cells, was semi-quantitatively scored as follows: 0 (absent sclerosis), 1 ($< 30\%$ of tumor area), 2 (30–60% of tumor area) and 3 ($> 60\%$ of tumor area). Central fibrotic scars, likely related to ischemic necrosis, were excluded from sclerosis assessment. Immunohistochemistry was performed on serial sections by using Immunoperoxidase technique (HRP Multimer), Ventana Automated Immunostainer System (Roche Diagnostics) and specific primary antibodies raised against Chromogranin A (clone LK2H10, dilution 1:1000), Synaptophysin (clone MRQ-40, dilution 1:200), pan-Cytokeratin AE1/AE3 (clone AE1/AE3, dilution 1:500), Ki-67 (clone MIB-1, dilution 1:100) (Novocastrol Laboratories Ltd.), VMAT1 (clone SLC18A1, dilution 1:500) and VMAT2 (clone OTI9E11, dilution 1:50) (Novus Biologicals), according to the manufacturers' instructions. Briefly, sections were deparaffinized and brought to water, subjected to heat-induced epitope retrieval and the reaction was evidenced by using Ultraview Universal Detection Kit and DAB 3'-5' as chromogen substrate (Roche Diagnostics). VMAT1 and VMAT2 immunoreactivity was semi-quantitatively evaluated on a scale from 0 to 6 (0, absent; 1, $< 10\%$ positive cells; 2, 10–19%; 3, 20–39%; 4, 40–59%;

Table 2 VMAT 1, VMAT 2, Sclerosis score and M-GAPP score in mutated and non-mutated (nm) patients

Patient N.	Diagnosis	Sclerosis score	M-GAPP score	V-MAT1 score	V-MAT 2 score	Genotype
1	HNPG	0	4	4	6	SDHD
2	HNPG	3	3	6	6	SDHC
3	HNPG	0	3	6	6	SDHC
4	HNPG	3	2	6	6	SDHD
5	HNPG	2	NA	5	6	SDHD
6	HNPG	1	3	5	6	SDHD
6	Bronchial PG	2	5	6	5	SDHD
7	HNPG	3	2	5	6	SDHD
8	HNPG	0	4	6	6	SDHD
9	HNPG	3	3	5	6	SDHD
10	HNPG	1	7	4	6	SDHD
11	HNPG	1	4	6	6	SDHC
12	PHEO	0	6	2	6	SDHB
13	PHEO	0	1	2	6	RET
14	Bilateral PHEO	0	5	0	6	SDHD
15	PHEO	0	NA	2	6	VHL
16	PHEO	1	6	6	6	VHL
17	PHEO	0	4	6	6	SDHD
18	Bilateral PHEO	2	2	6	6	RET
19	PHEO + APG	0	2	6	6	VHL
20	PHEO	2	5	6	6	SDHB
21	PHEO	0	0	6	6	RET
22	APG	1	2	6	5	SDHD
23	APG	1	6	6	6	SDHD
24	APG	0	4	6	6	SDHB
25	PHEO (Metastatic Behavior)	0	8	0	0	SDHB
26	HNPG	1	2	5	6	nm
27	HNPG	0	0	4	6	nm
28	HNPG	0	0	6	6	nm
29	HNPG	0	1	6	6	nm
30	HNPG	0	1	5	5	nm
31	HNPG	2	NA	3	6	nm
32	HNPG	0	0	6	6	nm
33	HNPG	0	1	6	6	nm
34	HNPG	1	1	6	6	nm
35	HNPG	0	0	4	6	nm
36	HNPG + APG + CTPG	0	0	6	6	nm
37	PHEO	0	4	5	0	nm
38	PHEO	0	4	3	6	nm
39	PHEO	0	1	2	6	nm
40	PHEO	0	1	3	6	nm
41	PHEO	0	1	3	6	nm
42	PHEO (Metastatic Behavior)	0	2	3	6	nm
43	PHEO	0	1	3	6	nm
44	PHEO	0	NA	5	6	nm
45	PHEO	1	1	5	6	nm
46	PHEO	0	2	6	6	nm
47	PHEO	0	4	5	6	nm
48	PHEO	0	2	6	6	nm

Table 2 (continued)

Patient N.	Diagnosis	Sclerosis score	M-GAPP score	V-MAT1 score	V-MAT 2 score	Genotype
49	PHEO	1	0	5	6	nm
50	PHEO	0	2	4	6	nm
51	APG	0	1	4	5	nm
52	Functioning APG	0	1	5	6	nm
53	Multiple APG	1	2	6	6	nm
54	Functioning APG (Metastatic Behavior)	0	1	6	6	nm
55	PHEO (Metastatic Behavior)	1	7	5	6	nm
55	PHEO (Metastasis)	NE	NE	6	6	nm

HNPG head & neck paraganglioma; *PHEO* pheochromocytoma; *PG* paraganglioma; *APG* abdominal paraganglioma; *CTPG* cervico-thoracic paraganglioma; *NA* not available; *NE* not evaluated (lymphnode metastasis)

5, 60–79%; 6, 80–100%) according to Fottner et al. [24]. Human adrenal gland tissue was used as positive control.

Genetic Analysis

Genetic counseling and genetic analyses were performed in all patients. As previously reported, DNA was extracted from peripheral blood leukocytes and analyzed for germ line mutations of all exons of *SDHD*, *SDHB*, *SDHC* and *SDHAF2* as well as of *RET* (exons 10, 11, 13–16) and *VHL* (all exons) genes, representing the most frequently involved genes in such tumors [7].

Statistical Analysis

Data are reported as means \pm SD. Chi-square and Mann-Whitney tests were used to analyze the different groups, VMAT1, VMAT2, tumor sclerosis and M-GAPP scores. Correlations between VMAT1, VMAT2, tumor sclerosis and M-GAPP scores were analyzed using Spearman's rank correlation coefficient or Spearman's ρ . $p < 0.05$ was considered significant.

All statistical analyses were performed using the Prism-GraphPad 8 (version 8.3.1) software.

Results

PGs: Clinical and Histological Characterization

The clinical diagnosis of PG was confirmed in 30/57 tumors (52.6%) from 29/55 patients (52.7%), mostly HNPGs (N=22), then abdominal PGs (APGs, N=7) and a bronchial PG. Data collection and patients' clinical history revealed metachronous tumors in 3 patients, respectively affected by multiple APGs, by a HNPG followed by an APG and by a cervico-thoracic PG, or by a HNPG followed by a bronchial PG (Table 2).

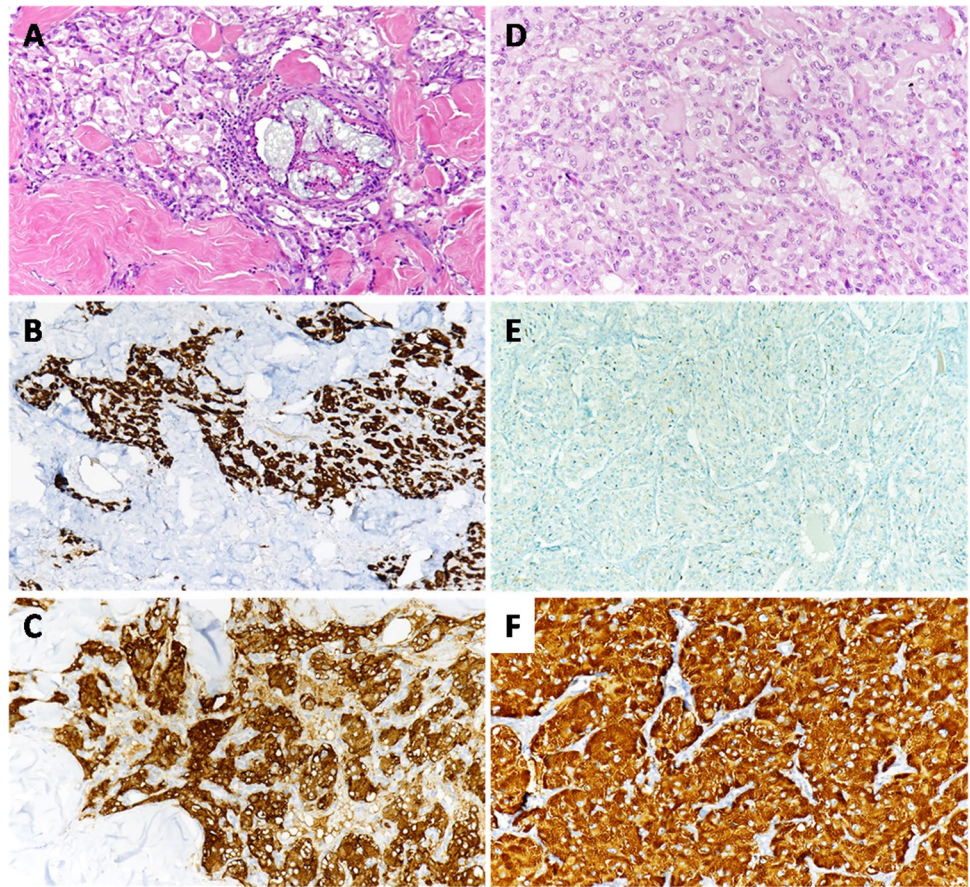
Metastatic behavior was shown in a 35-year-old man (patient N. 54, Table 1) affected by APGL; at 7-year follow-up, he showed splenic and abdominal lymph node metastases that were surgically removed, and he is alive at 11-year follow-up (Table 2).

By histology, all PGs showed features typical for neuroendocrine neoplasia; they were mostly composed by uniform cells with eosinophilic cytoplasm and arranged in a "zellballen" pattern, i.e., cell nests delimited by sustentacular cells within a fibrovascular stroma (Fig. 1). Larger (clear or spindle) cells, nuclear pleomorphism and/or a diffuse growth pattern were observed in few cases (*next paragraph*). Neoplastic capsular infiltration and/or angioinvasion were detected in a minority of cases (N=8); most tumors were well delimited by a fibrous capsule.

M-GAPP score was evaluated in 28/30 (93.33%) PGs (Table 2), two patients lacking diuresis data. Most of them (24/28; 85.7%) showed a zellballen architecture; large and irregular nests were observed in the remaining 4 (14.3%) tumors. Comedo-type necrosis was found in one case. The ki-67 proliferative index was $< 1\%$ in 14 (50%) PGs, between 1% and 3% in 11 (39.3%) and $> 3\%$ in 3 (10.7%). The tumor with metastatic behavior showed M-GAPP score 1; it was characterized by norepinephrine secretion, Ki-67 proliferating index $< 1\%$ and no pseudo-rosette, comedo-type necrosis, capsular and/or vascular infiltration.

Tumor sclerosis was found in 15/30 (50%) PGs (11 HNPGs, 3 APGs and the bronchial PG) (Table 2). Sclerosis was characterized by broad bands of hyaline fibrous tissue delimiting nests or cords of tumor cells (Fig. 1). At the periphery of the tumor, fibrosis might mimic an infiltrative growth pattern whereas in the neoplastic core the embedded cells might show moderate atypia or even nuclear pleomorphism. High (≥ 2) sclerosis score was found in 7 PGs (6 HNPGs and the bronchial PG), only two of them corresponding to functioning tumors. No correlation was found between multiple tumors and sclerosis, the 3 metachronous PGs showing sclerosis score 2, 1 or 0, respectively.

Fig. 1 Sclerosis and VMAT immunoreactivity in paragangliomas and pheochromocytomas. **A–C** A head and neck paraganglioma showing **(A)** high (score 3) sclerosis, high (score 6) VMAT1 **(B)** and VMAT2 **(C)** immunoreactivity. **D–F** A pheochromocytoma with **(D)** no (score 0) sclerosis, no (score 0) VMAT1 **(E)** immunoreactivity and high (score 6) VMAT2 **(F)** immunostaining (**A, D**, Hematoxylin and Eosin staining; **B, C, E, F**, Immunoperoxidase staining and Hematoxylin counterstaining; original magnification: 10x)



By immunohistochemistry, all PGs showed Chromogranin A, Synaptophysin and no pan-Cytokeratin (AE1/AE3) expression. VMAT1 and VMAT2 expression was detected in all PGs (Fig. 1). VMAT1 score 6 was found in 11/22 (50%) HNPGs, in 5/7 (71%) APGs and in the bronchial PG (the latter one from a patient with a previous HNPG showing VMAT1 score 6). A higher VMAT1 (4–6 score range) expression was detected in 95.5% of HNPGs, in 100% of APGs and in the bronchial PG. Semi-quantitative analysis of VMAT2 expression showed a strong immunoreactivity (score 6) in all PGs. In the metastatic APG, both VMAT2 and VMAT1 displayed the highest (score 6) expression (Table 2).

Genetic analyses showed a known germ-line mutation involving an SDHx gene in 14/30 (46,66%) patients with PGs, including 11 patients affected by HNPGs and 3 patients with APG (Table 2). One of the three patients with multiple tumors (a HNPG with a metachronous bronchial PG) showed an SDHD gene mutation. No known germ-line mutation was identified in the patient with metastatic behavior of PG. By comparing mutated vs. non-mutated patients, we found that sclerosis frequency ($p=0.048$) and mean score ($p=0.020$) were significantly higher in PGs from patients with a mutated status (Fig. 2). Also M-GAPP score

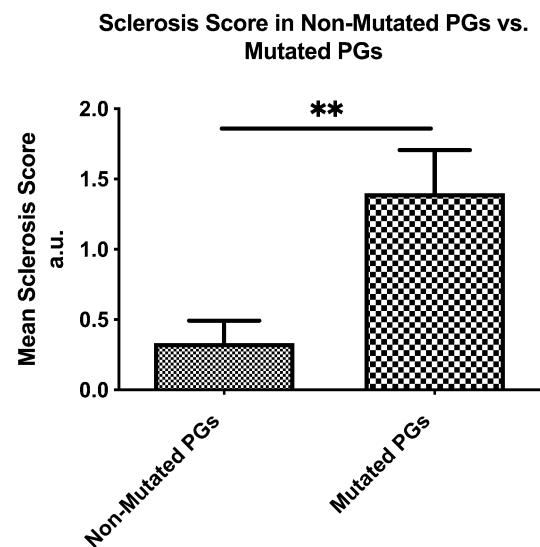


Fig. 2 Sclerosis score in paragangliomas from non-mutated vs. mutated patients: independent samples Mann–Whitney U test was applied for assessing mean score differences. Mean sclerosis score is significantly higher in PGs of patients with a mutated status ($p < 0.05$)

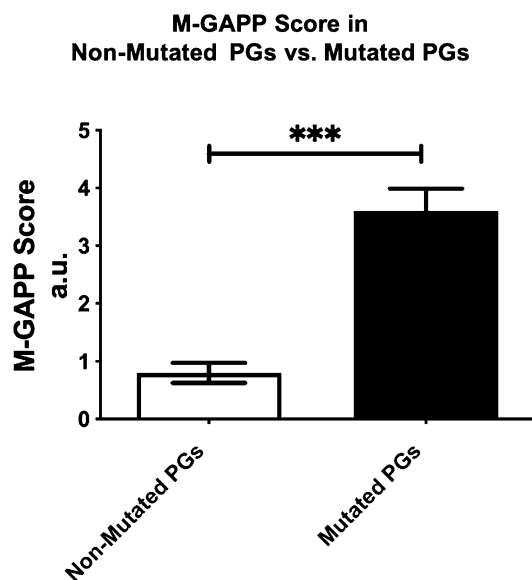


Fig. 3 M-GAPP score in paragangliomas from non-mutated vs. mutated patients. M-GAPP mean score was significantly higher in PGs from mutated patients. Independent samples Mann–Whitney U test was applied for assessing mean score differences. * $p < 0.05$

was significantly higher in mutated vs. non-mutated PGs ($p < 0.0001$) by Mann–Whitney test (Fig. 3). No statistically significant difference was found in VMAT1 frequency or in VMAT1 score values between mutated and non-mutated PGs.

PHEOs: Clinical and Histological Characterization

PHEO was diagnosed in the remaining 27 tumors (47.4%) from 26/55 patients (47.3%) (Table 1). Multiple tumors were diagnosed in 3 patients, two of them showing synchronous PHEOs and the third one a metachronous APG (Table 2). At follow-up, a metastatic behavior was displayed in 3 patients. A young woman (patient N. 25, Table 1), diagnosed with PHEO at 18 years of age, developed liver metastases and peritoneal carcinosis two years after diagnosis and died few months later. Another woman was diagnosed with a PHEO at 45 years of age (N. 42, Table 1) and presented splenic, omental, and abdominal lymph node metastases at 7-year follow-up; she underwent metastases resection and is alive at 9-year follow-up. The third patient was a 55 y.o. man (N. 55, Table 1) that developed abdominal and omental lymph node metastases two years after resection of a PHEO; he is alive at 7-year follow-up.

By histology, all PHEOs showed the typical features of a neuroendocrine neoplasia (Fig. 1). Larger clear or spindle cells, nuclear pleomorphism and/or a diffuse pattern of growth were observed in few PHEOs (*see next paragraph*;

Figs. 1,4). Neoplastic capsular infiltration and/or angioinvasion were detected in 11 PHEOs.

M-GAPP score could be calculated in 24/27 (88,9%) PHEOs; in the remaining three tumors, secretion data were not available ($N=2$) or the tumor was represented by a lymph node metastasis (Table 2). Azellballen architecture was shown in 10 PHEOs (41.67%), large and irregular nests in 11 (45.83%) tumors and pseudo-rosettes in the remaining 3 (12.5%). In 2 (8.3%) cases, comedo-type necrosis was found. The ki-67 proliferative index was $< 1\%$ in 10 (41.67%) cases, 1–3% in 10 (41.67%) and $> 3\%$ in 4 (16.66%). Two out of the three tumors with metastatic behavior showed a high (7 and 8, respectively) M-GAPP score value, the third one had M-GAPP score 2; the first two were characterized by pseudo-rosettes, comedo-type necrosis, capsular and/or vascular infiltration, high proliferative index and mitosis presence (Figs. 4 and 5), whereas the third one showed irregular large nests and capsular invasion.

No correlation was found between the presence of multiple localizations or metastatic behavior and sclerosis; only a bilateral PHEO showed a score 2 value.

By immunohistochemistry, all PHEOs showed Chromogranin A and Synaptophysin expression with no pan-Cytokeratin (AE1/AE3) immunostaining. VMAT1 and VMAT2 were detected in all but two PHEOs (92.6%) (Table 2). In all VMAT1 and VMAT2 immunoreactive PHEOs, score 6 VMAT2 immunoreactivity and variable VMAT1 score were detected. The higher (4–6) VMAT1 scores were found in 59.3% of PHEOs, with score 6 in 33% of them. As to PHEOs with metastatic behavior, both VMATs were negative in one case (Fig. 4) whereas the remaining two showed VMAT2 score 6 and variable (3 or 6, respectively) VMAT1 score (Table 2).

Genetic analyses of patients affected by PHEO showed a mutated status in 11/26 (42.31%) patients (Table 2). RET and SDHD gene mutations were respectively detected in the two patients with bilateral PHEOs, whereas SDHB mutation was found in the young woman with metastatic behavior and fatal disease. Sclerosis ($p=0.24$) and M-GAPP score ($p=0.09$) were not statistically different in mutated vs. non-mutated PHEOs.

Overall Series and Comparison of PGs vs. PHEOs

Sclerosis was found in 21/57 (36.8%) tumors. Sclerosis frequency and sclerosis score were significantly different in PGs vs. PHEOs ($p=0.03$ and $p=0.04$, respectively, Fig. 6); sclerosis was mainly present in PGs (15/30 PGs vs. 6/27 PHEOs) and the highest (2 and 3) sclerosis scores were found in 9 tumors, 7/9 corresponding to PGs (Table 2).

Also VMAT1 score was significantly higher in PGs vs. PHEOs ($p=0.006$; Fig. 7).

Fig. 4 Sclerosis and VMAT immunoreactivity in two pheochromocytomas with metastatic behavior. The first A–C pheochromocytoma showed no sclerosis (A), no VMAT1 (B) or VMAT2 (C) immunoreactivity. The latter one D–F was characterized by a low (score 1) sclerosis (D), high (score 5) VMAT1 (E) and (score 6) VMAT 2 (F) immunoreactivity (A, D, Hematoxylin and Eosin staining; B, C, E, F, Immunoperoxidase staining and Hematoxylin counterstaining; original magnification: 10x)

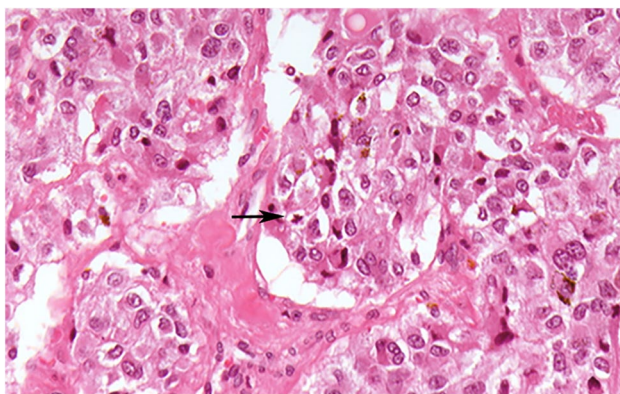
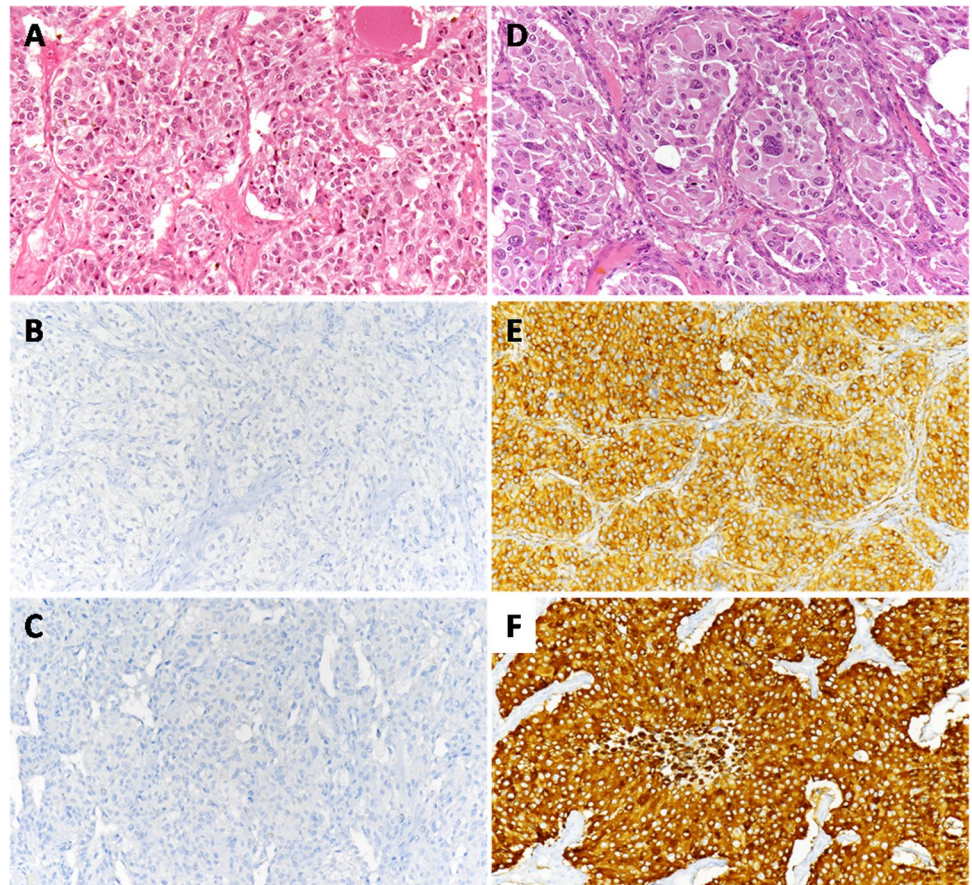


Fig. 5 Mitotic activity in a pheochromocytoma with metastatic behavior. A mitotic figure is evidenced (arrow) in a PHEO showing metastatic behavior at follow-up (Hematoxylin and Eosin staining; original magnification: $\times 20$)

M-GAPP mean score did not statistically differ between PGs (mean score = 2.25) and PHEOs (mean score = 2.96; $p=0.28$), whereas M-GAPP scores correlated with sclerosis ($p=0.029$) and the M-GAPP mean score was significantly higher in sclerosing tumors vs. non-sclerosing tumors ($p=0.0231$) (Fig. 8B). M-GAPP score was calculated in 52

tumors; 34 (65.4%) showed a zellballen architecture, 15/52 (28.8%) large and irregular nests and the remaining 3/52 (5.8%) pseudo-rosettes. In 3/52 (5.8%) cases, comedo-type necrosis was found.

The ki-67 proliferative index was $< 1\%$ in 24/52 (46.2%) cases, between 1% and 3% in 21/52 (40.4%) and $> 3\%$ in 7/52 (13.4%). As expected, a strong correlation was found between Ki-67 index and M-GAPP score by Spearman’s rank correlation with 95% confidence interval ($p < 0.0001$), whereas Ki67 index did not significantly differ between PGs and PHEOs ($p=0.71$) and it did not correlate with sclerosis. Two of the 4 patients with metastatic behavior showed a $> 3\%$ Ki67 index and the remaining two a $< 1\%$ Ki67 index; such a small number of observations did not allow a powerful statistical analysis as to the risk of metastasis.

Genetic analyses identified 25/55 (45.5%) patients with a germ line mutation; in 19/25 (76%) the mutation involved *SDHx* genes (4 *SDHB*, 3 *SDHC*, 12 *SDHD*), in 3 (12%) the *RET* gene and in the remaining 3 (12%) the *VHL* gene (Table 2). By comparing tumor sclerosis and genetic data, we found that sclerosis score was higher in mutated patients’ tumors as compared to non-mutated ones ($p=0.014$) (Fig. 9). We also found a correlation between sclerosis score and mutations by Spearman’s test ($p=0,0027$). Sclerosis

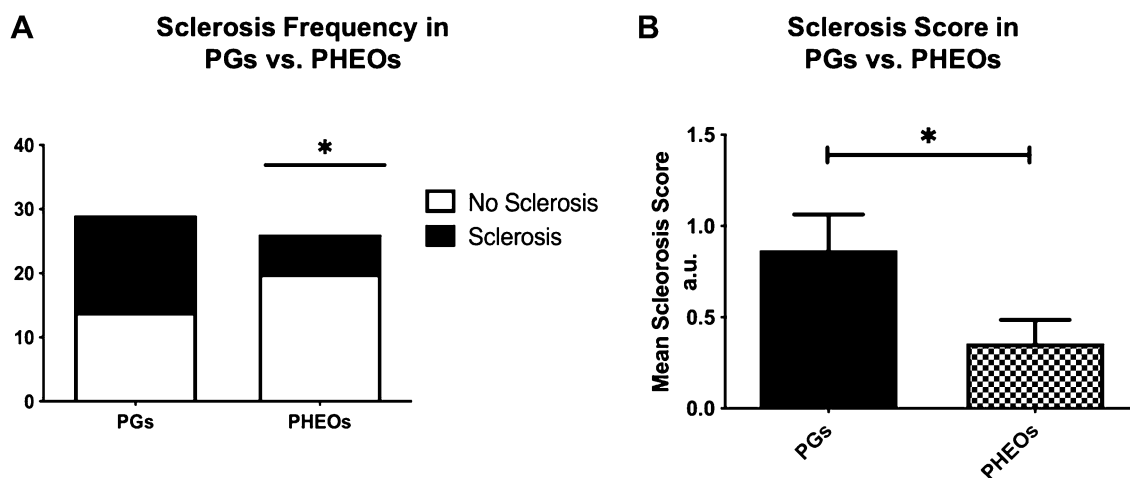


Fig. 6 Frequency (A) and score (B) of sclerosis in paragangliomas vs. pheochromocytomas: frequency and mean score were higher in Paragangliomas as compared to Pheochromocytomas. Frequency was

investigated by Chi-square test; independent samples Mann–Whitney U test was used for assessing mean score differences. * $p < 0.05$

was more frequently associated to germ-line mutations ($N = 14/25$, 56.7%; $p = 0.01$) and to the diagnosis of PG ($N = 11/14$, 78.6%), most of the patients ($N = 8/11$, 72.7%) being affected by HNPG (Table 2).

As to the VMAT1 score values and the mutated status, score 6 was more frequently detected in mutated patients' tumor as compared to non-mutated ones ($p < 0.01$), whereas VMAT1 mean score did not significantly differ (Fig. 10). As expected, no difference between mutated and non-mutated patients was observed for VMAT2 expression that was highly expressed (score 6) in most cases ($N = 55/57$ tumors).

M-GAPP mean score value was significantly higher in mutated cases as compared to non-mutated ones ($p < 0.0001$) (Fig. 8 A) and a strong correlation was found between mutated patients and M-GAPP score ($p < 0.0001$), whereas Ki-67 index did not correlate with mutation status.

The presence of mutations was not related to the functioning phenotype or to the diagnosis of PG or PHEO.

As to multiple tumors, in 4/6 (66.7%) cases we found a known germ-line mutation, involving RET or SDHD gene in the two patients with PHEOs, SDHD or VHL gene in the other two patients with PGs.

In the 4 patients with metastatic behavior, a mutated status (an SDHB gene mutation) was found only in the 18-year-old woman with fatal outcome.

Discussion

In the present study, we investigated 57 neuroendocrine tumors (30 PGs and 27 PHEOs) in 55 patients from a single Center. We found that tumor sclerosis and VMAT1 expression were significantly higher in mutated patients affected

by PG. Tumors with sclerosis score ≥ 2 represented 16% of cases (7 HNPGs and 2 PHEOs) and a germ-line mutation was found in 8/9. Furthermore, we showed that a higher M-GAPP score was correlated with the presence of mutations and with tumor sclerosis. These results confirm that germ-line mutations may help in early diagnosis and in identifying asymptomatic patients or patients with tumor susceptibility that deserve closer follow-up or familial counseling [1]. It has been previously shown that PGs and PHEOs from patients with SDHA, SDHB and SDHC mutations show higher biological aggressiveness and SDHB mutations have been associated with the presence of metastasis [3, 25, 26]. In our study we could not analyze this latter aspect because of the limited number ($N = 4$) of tumors with metastatic behavior, only one of them carrying an SDHB mutation in a young patient with fatal disease.

We did find that VMAT1 score was higher in PGs than in PHEOs ($p = 0.0006$). These findings are at least partially according to another study showing higher VMAT1 (and VMAT2) transporter mRNA expression in PGs than in PHEOs, by means of quantitative real time PCR [27]. However, conflicting results have been reported on this topic. Previous *in vivo* and *in vitro* studies on mammalian (rat or bovine) cells and on normal human tissues have shown that VMAT1 and VMAT2 are predominantly expressed by adrenal chromaffin cells and by parasympathetic paraganglia, respectively [28]. Fottner et al. found most VMAT-1-negative tumors to be represented by parasympathetic PGs and to have extra-adrenal localization [24]. Although we do not have a straightforward explanation for such discrepancies, it must be pointed out that the present study investigated one of the widest reported cohorts on this topic, providing further data to the knowledge of this controversial issue and

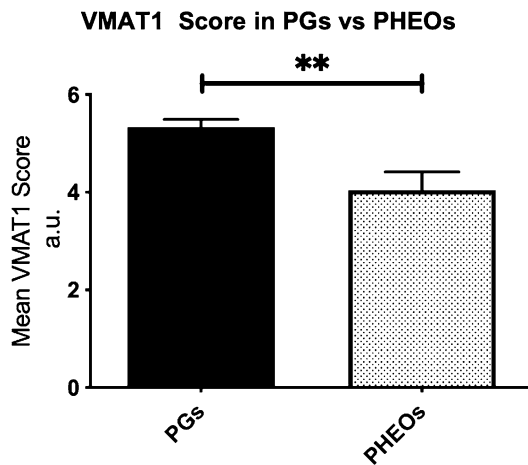


Fig. 7 Comparison of VMAT1 score in paragangliomas vs. pheochromocytomas. VMAT1 mean score was significantly higher in Paragangliomas. The independent samples Mann–Whitney U test was used for assessing mean score differences. ** $p < 0.01$

underlying the complexity of these neuroendocrine tumours [1]. In a previous study we also observed that VMAT1-2 expression does not constitute a limiting factor for MIBG uptake [17]; also other Authors did not find any correlation between MIBG and VMAT1 expression and altogether these results might partially explain the variable diagnostic significance of these radiotracers [29].

In this series, the highest VMAT1 score (i.e., score 6) was more frequently observed in mutation-bearing patients' tumors ($p < 0.01$). This topic could be worthy of further investigation. In a previous study, no significant difference in VMAT1 expression was found in 24 mutated versus 33 non-mutated PGs [29]. In this latter series, a different immunoreactivity score, combining the percentage of tumor cells with positive staining and the intensity of immunostaining, was used and additional (MAX and NF1) genes were also investigated.

Nowadays all PHEOs and PGs are considered to have metastatic potential, suggesting a risk stratification based on histological and clinical features including invasion of capsule and of blood vessels, peculiar architectural patterns, high mitotic count or proliferation index, tumor site and hormone secretory profile [3, 15, 30]. For this retrospective study, we have been using the M-GAPP scoring system that represents one of the most widely adopted scoring systems for PGs/PHEOs in the last decade [15, 31]. M-GAPP score evaluates the histological pattern, the presence of comedo-type necrosis, of capsular/vascular invasion, the Ki67 labeling (or proliferation index), the catecholamine secretion and the SDH gene status that is considered a high-risk factor for metastasis [15, 21, 25, 32, 33]. SDHB immunohistochemistry is considered a reliable tool for detecting SDH-x (SDHB, SDHC, and SDHD) germ-line mutations on FFPE tumors [21–23], but a heterogeneous SDHB

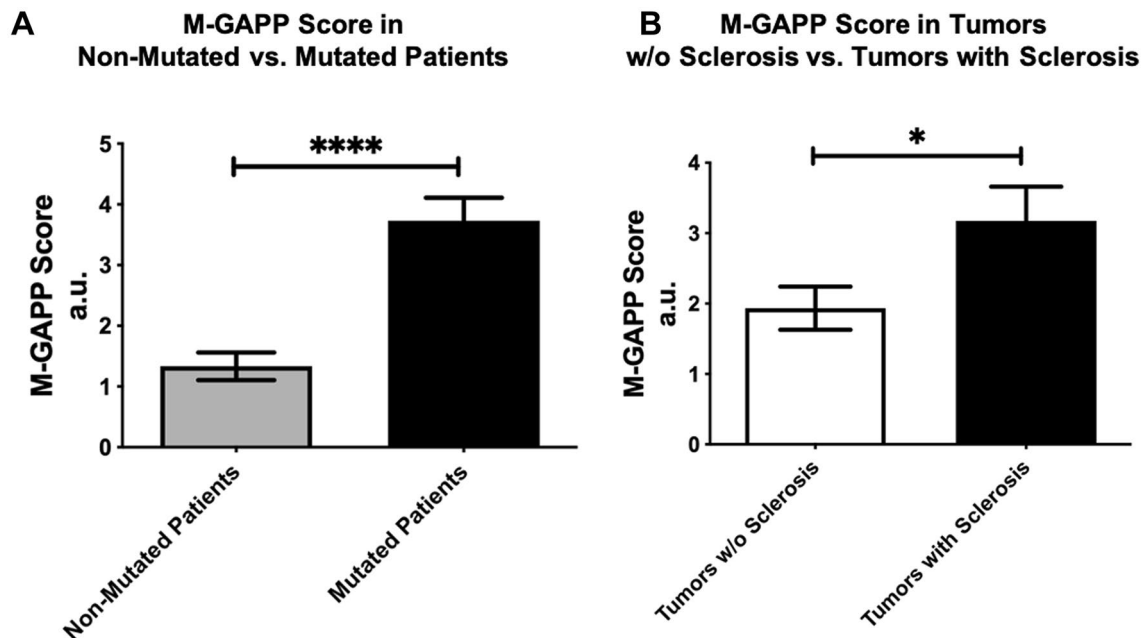


Fig. 8 M-GAPP score in tumors from non-mutated vs. mutated patients (A) and in tumors with or without (w/o) sclerosis (B). M-GAPP score was significantly higher in tumors from patients bear-

ing a germ-line mutation such as in tumors with Sclerosis Chi-square test for frequency was used. * $p < 0.05$

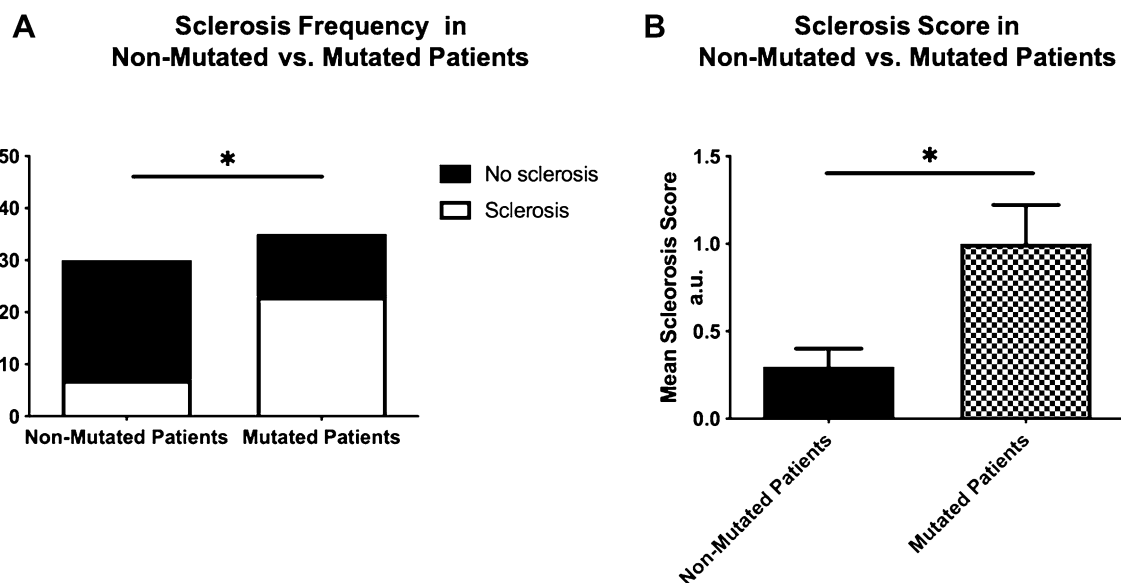


Fig. 9 Frequency (A) and score (B) of sclerosis in tumors from non-mutated vs. mutated patients. Sclerosis was higher and more frequent in tumors from patients with a mutated status. Chi-square test for fre-

quency was used; independent samples Mann–Whitney U test was applied for assessing mean score differences. * $p < 0.05$, *** $p < 0.001$

immunoreactivity requires SDH molecular genetic testing such as a subset of SDHB-immunonegative tumors might harbor other mutations (e.g., for VHL and NF1 genes) [23]. In our study we replaced immunohistochemistry for SDHB with genetic evaluation which was available to us. We found a strong correlation between Ki-67 index and M-GAPP score ($p < 0.0001$); this result was predictable because Ki67 index is a parameter of this score [19].

In the present series including 4 tumors with metastatic behavior, a high (i.e., 7 and 8, respectively) M-GAPP score was shown in 2 of them; such a small number does not allow any further consideration.

A strong correlation was found between mutation-bearing patients' tumors and M-GAPP score ($p < 0.0001$). These results could be predictable since SDHx genes mutation represents an important parameter in the score, and 7/9 sclerosing tumors had mutations in SDHx genes. We also observed that M-GAPP score correlated with tumor sclerosis ($p = 0.029$). Sclerosing PGs constitute a minority of cases that may mimic a malignant neoplasia [11–14]. Our data point out to sclerosis not only as a peculiar histological feature that must be correctly considered in such tumors for the differential diagnosis from malignant/aggressive neoplasia, but also a possible histological marker of tumor susceptibility and patient vulnerability. Although our results need to be furtherly confirmed, tumor sclerosis could be an appealing candidate to enter a scoring system. Indeed, it is well known that myofibroblasts may play a role in the stromal response of the host against neoplasm or in the regulation of tumor

growth [34]. As early as in 2007 Kuroda N. at al. identified the myofibroblasts as the third stromal component in PG [35]. Further studies investigated the role of the microenvironment (using fibroblasts co-culture) on *SDHB*-silenced cells (monolayer and spheroid) and demonstrated that fibroblasts enhance collective migration/ invasion and metastatic potential [36, 37]. And in small intestinal neuroendocrine tumors (NETs) accumulating evidence suggests that the tumour microenvironment plays a pivotal role not only in the neoplastic progression but also in the pathogenesis of their fibrotic complications [38]. Significant alterations are usually observed in the extracellular matrix of small intestinal NETs, and the biologic underpinnings of focal desmoplasia is a common feature of these tumours. Moreover, in pulmonary NETs, the extent of extracellular matrix remodelling has been described to be grade-dependent and associated with increased tumour size and nodal metastases [39, 40]. In both small intestinal and bronchopulmonary NETs, a dynamic crosstalk between neoplastic cells and reactive stroma regulates the growth and tumour progression, and intensive research is currently underway to therapeutically exploit the vulnerabilities of such a molecular interplay [41].

In conclusion, higher tumor sclerosis, M-GAPP and VMAT1 scores were associated to germ-line mutations in PGs; it could be hypothesized that sclerosis might represent a histological marker of tumor susceptibility in PGs, prompting to genetic investigation, whereas in our series we could not demonstrate any straightforward correlation between M-GAPP score and tumor behavior.

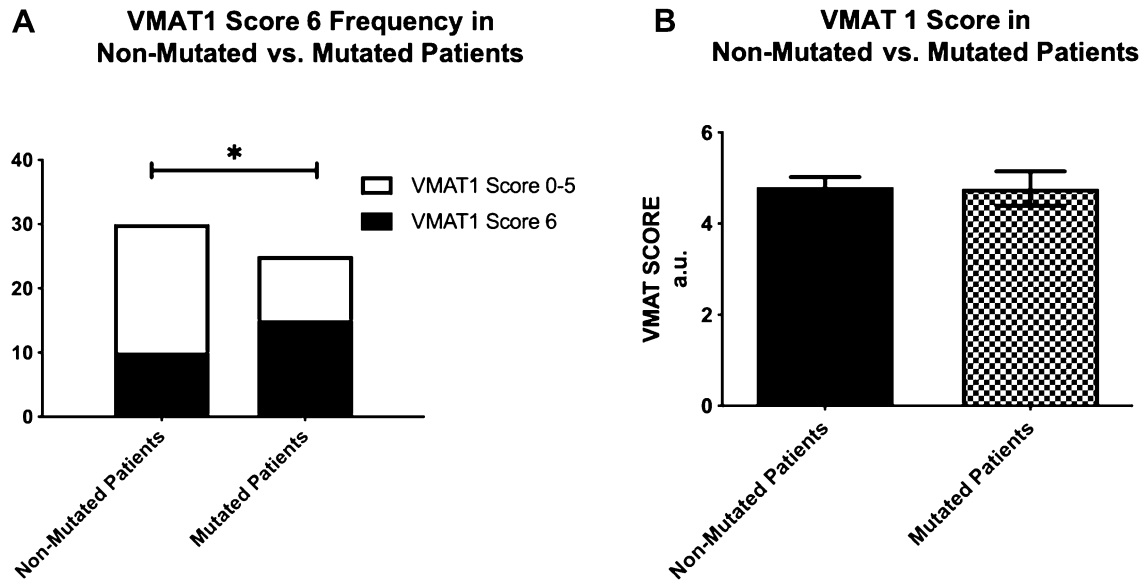


Fig. 10 VMAT1 score 6 frequency (A) and VMAT1 mean score (B) in tumors from non-mutated vs. mutated patients. VMAT1 score 6 frequency and VMAT1 mean score were higher in mutated patients.

Chi-square test for frequency was used; independent samples Mann-Whitney U test was applied for assessing mean score differences. * $p < 0,01$

Acknowledgements The Authors wish to thank Mrs. Alice Cocco, B.Sc., for excellent technical assistance.

Author Contributions All authors contributed to the study conception and design. The first draft of the manuscript was written by AP and all authors commented on previous versions of the manuscript. All authors read and approved the final manuscript. Conceptualization: AP, AB, GB, FB; Methodology: AP, AB, GB; Formal analysis and investigation: AP, AB, IB, IDS, BB, DL, LT, SC, CC; Writing—original draft preparation: AP; Writing—review and editing: AP, AB, DA; Funding acquisition: GB; Resources: GB; Supervision: FB, GB; GM, MF.

Funding From Italian Ministry of Research and Health to G. Bernini.

Data Availability All data generated or analyzed during this study are included in the manuscript.

Code Availability Not applicable.

Declarations

Conflict of interest The authors declare that they have no conflict of interest.

Ethical Approval The study was approved by the Institutional Ethics Committee and conformed to the Declaration of Helsinki.

Consent to Participate The informed consent was obtained from each patient.

Consent for Publication All co-authors have approved this paper and have given the consent for publication.

References

1. Neumann HPH, Young WF Jr, Eng C. Pheochromocytoma and paraganglioma. *N Engl J Med.* 2019;381(6):552–65.
2. Pang Y, Liu Y, Pacak K. Pheochromocytomas and paragangliomas: from genetic diversity to targeted therapies. *Cancers (Basel).* 2019;11:436.
3. Turchini J, Cheung VKY, Tischler AS, De Krijger RR, Gill AJ. Pathology and genetics of pheochromocytoma and paraganglioma. *Histopathology.* 2018;72:97–105.
4. Favier J, Amar L, Gimenez-Roqueplo AP. Paraganglioma and pheochromocytoma: from genetics to personalized medicine. *Nat Rev Endocrinol.* 2015;11:101–11.
5. Costa MH, Ortiga-Carvalho TM, Violante AD, Vaisman M. Pheochromocytomas and paragangliomas: clinical and genetic approaches. *Front Endocrinol (Lausanne).* 2015;17:6:126. <https://doi.org/10.3389/fendo.2015.00126>.
6. Sen I, Young WF Jr, Kasperbauer JL, Polonis K, Harmsen WS, Colglazier JJ, DeMartino RR, Oderich GS, Kalra M, Bower TC. Tumor-specific prognosis of mutation-positive patients with head and neck paragangliomas. *J Vasc Surg.* 2020;71:1602-12.e2.
7. Bacca A, Sellari Franceschini S, Carrara D, Bernini M, Zampa V, Taddei S, Miccoli P, Congregati C, Simi P, Ferrari M, Bernini G. Sporadic or familial head neck paragangliomas enrolled in a single center: clinical presentation and genotype/phenotype correlations. *Head Neck.* 2013;35:23–7.
8. Alevizaki M, Stratakis CA. Multiple endocrine neoplasias: advances and challenges for the future. *J Intern Med.* 2009;266:1–4.
9. Buffet A, Burnichon N, Favier J, Gimenez-Roqueplo AP. An overview of 20 years of genetic studies in pheochromocytoma and paraganglioma. *Best Pract Res Clin Endocrinol Metab.* 2020;34:101416. <https://doi.org/10.1016/j.beem.2020.101416>.
10. Tischler AS, de Krijger RR, Gill A, Kawashima A, Kimura N, Komminoth P. Tumours of the adrenal medulla and extra-adrenal paraganglia. In: Lloyd RV, Osamura RY, Kloppel G, Rosai J,

- editors. WHO classification of tumours of endocrine organs, vol. 4. Lyon: IARC Press; 2017. p. 179–207.
11. Javidiparsijani S, Brickman A, Lin DM, Rohra P, Ghai R, Bitterman P, Reddi V, Al-Khudari S, Gattuso. Is regional lymph node metastasis of head and neck paraganglioma a sign of aggressive clinical behavior: a clinical/pathologic review. *Ear Nose Throat J.* 2021;100:447–53.
 12. Plaza JA, Wakely PE Jr, Moran C, Fletcher CD, Suster S. Sclerosing paraganglioma: report of 19 cases of an unusual variant of neuroendocrine tumor that may be mistaken for an aggressive malignant neoplasm. *Am J Surg Pathol.* 2006;30:7–12.
 13. Santi R, Franchi A, Saladino V, Trovati M, Cenacchi G, Squadrelli-Saraceno M, Nesi G. Sclerosing paraganglioma of the carotid body: a potential pitfall of malignancy. *Head Neck Pathol.* 2015;9:300–4.
 14. Ng E, Duncan G, Choong AM, Francis L, Foster W, Kruger A. Sclerosing paragangliomas of the carotid body: a series of a rare variant and review of the literature. *Ann Vasc Surg.* 2015;29(7):1454.e5. <https://doi.org/10.1016/j.avsg.2015.04.083>.
 15. Wang Y, Li M, Deng H, Pang Y, Liu L, Guan X. The systems of metastatic potential prediction in pheochromocytoma and paraganglioma. *Am J Cancer Res.* 2020;10:769–80.
 16. Henry JP, Botton D, Sagne C, Isambert MF, Desnos C, Blanchard V, Raisman-Vozari R, Krejci E, Massoulie J, Gasnier B. Biochemistry and molecular biology of the vesicular monoamine transporter from chromaffin granules. *J Exp Biol.* 1994;196:251–62.
 17. Bacca A, Pucci A, Lorenzini D, Chiacchio S, Volterrani D, Ferrari M, Sellari Franceschini S, Materazzi G, Basolo F, Bernini G. Vesicular monoamine transporters expression in pheochromocytomas and paragangliomas according to scintigraphy and positron emission tomography behavior. *Q J Nucl Med Mol Imaging.* 2021;65:396–401.
 18. Bombardieri E, Maccauro M, De Deckere E, Savelli G, Chiti A. Nuclear medicine imaging of neuroendocrine tumours. *Ann Oncol.* 2001;12(Suppl 2):51–61.
 19. Koh JM, Ahn SH, Kim H, Kim BJ, Sung TY, Kim YH, Hong SJ, Song DE, Lee SH. Validation of pathological grading systems for predicting metastatic potential in pheochromocytoma and paraganglioma. *PLoS One.* 2017;12:e0187398.
 20. Kimura N, Takayanagi R, Takizawa N, Itagaki E, Katabami T, Kakoi N, Rakugi H, Ikeda Y, Tanabe A, Nigawara T, Ito S, Kimura I, Naruse M, Phaeochromocytoma Study Group in Japan. Pathological grading for predicting metastasis in phaeochromocytoma and paraganglioma. *Endocr Relat Cancer.* 2014;21:405–14.
 21. Lenders JW, Duh QY, Eisenhofer G, Gimenez-Roqueplo AP, Grebe SK, Murad MH, Naruse M, Pacak K, Young WF Jr, Endocrine Society. Pheochromocytoma and paraganglioma: an endocrine society clinical practice guideline. *J Clin Endocrinol Metab.* 2014;99:1915–42.
 22. van Nederveen FH, Gaal J, Favier J, Korpershoek E, Oldenburg RA, de Bruyn EM, Sleddens HF, Derckx P, Rivière J, Dannenberg H, Petri BJ, Komminoth P, Pacak K, Hop WC, Pollard PJ, Mannelli M, Bayley JP, Perren A, Niemann S, Verhofstad AA, de Bruine AP, Maher ER, Tissier F, Méatchi T, Badoual C, Bertherat J, Amar L, Alataki D, Van Marck E, Ferrau F, François J, de Herder WW, Peeters MP, van Linde A, Lenders JW, Gimenez-Roqueplo AP, de Krijger RR, Dinjens WN. An immunohistochemical procedure to detect patients with paraganglioma and phaeochromocytoma with germline SDHB, SDHC, or SDHD gene mutations: a retrospective and prospective analysis. *Lancet Oncol.* 2009;10:764–71. [https://doi.org/10.1016/S1470-2045\(09\)70164-0](https://doi.org/10.1016/S1470-2045(09)70164-0).
 23. Papatomas TG, Oudijk L, Persu A, Gill AJ, van Nederveen F, Tischler AS, Tissier F, Volante M, Matias-Guiu X, Smid M, Favier J, Rapizzi E, Libe R, Currás-Freixes M, Aydin S, Huynh T, Lichtenauer U, van Berkel A, Canu L, Domingues R, Clifton-Bligh RJ, Bialas M, Vikkula M, Baretton G, Papotti M, Nesi G, Badoual C, Pacak K, Eisenhofer G, Timmers HJ, Beuschlein F, Bertherat J, Mannelli M, Robledo M, Gimenez-Roqueplo AP, Dinjens WN, Korpershoek E, de Krijger RR. SDHB/SDHA immunohistochemistry in pheochromocytomas and paragangliomas: a multicenter interobserver variation analysis using virtual microscopy: a Multinational Study of the European Network for the Study of Adrenal Tumors (ENS@T). *Mod Pathol.* 2015;28:807–21. <https://doi.org/10.1038/modpathol.2015.41>.
 24. Fottner C, Helisch A, Anlauf M, Rossmann H, Musholt TJ, Kreft A, Schadmand-Fischer S, Bartenstein P, Lackner KJ, Klöppel G, Schreckenberger M, Weber MM. 6-18F-fluoro-L-dihydroxyphenylalanine positron emission tomography is superior to 123I-metaiodobenzyl-guanidine scintigraphy in the detection of extraadrenal and hereditary pheochromocytomas and paragangliomas: correlation with vesicular monoamine transporter expression. *J Clin Endocrinol Metab.* 2010;95:2800–10.
 25. Lee H, Jeong S, Yu Y, Kang J, Sun H, Rhee JK, Kim YH. Risk of metastatic pheochromocytoma and paraganglioma in SDHx mutation carriers: a systematic review and updated meta-analysis. *J Med Genet.* 2020;57:217–25.
 26. Crona J, Lamarca A, Ghosal S, Welin S, Skogseid B, Pacak K. Genotype-phenotype correlations in pheochromocytoma and paraganglioma: a systematic review and individual patient meta-analysis. *Endocr Relat Cancer.* 2019;26:539–50.
 27. Saveanu A, Muresan M, De Micco C, Taieb D, Germanetti AL, Sebag F, Henry JF, Brunaud L, Enjalbert A, Weryha G, Barlier A. Expression of somatostatin receptors, dopamine D2 receptors, noradrenaline transporters, and vesicular monoamine transporters in 52 pheochromocytomas and paragangliomas. *Endocr Relat Cancer.* 2011;18:287–300.
 28. Erickson JD, Schafer MK, Bonner TI, Eiden LE, Weihe E. Distinct pharmacological properties and distribution in neurons and endocrine cells of two isoforms of the human vesicular monoamine transporter. *Proc Natl Acad Sci USA.* 1996;93:5166–71.
 29. van Berkel A, Rao JU, Lenders JW, Pellegata NS, Kusters B, Piscaer I, Hermus AR, Plantinga TS, Langenhuijsen JF, Vriens D, Janssen MJ, Gotthardt M, Timmers HJ. Semiquantitative 123I-metaiodobenzylguanidine scintigraphy to distinguish pheochromocytoma and paraganglioma from physiologic adrenal uptake and its correlation with genotype-dependent expression of catecholamine transporters. *J Nucl Med.* 2015;56:839–46.
 30. Cho YY, Kwak MK, Lee SE, Ahn SH, Kim H, Suh S, Kim BJ, Song KH, Koh JM, Kim JH, Lee SH. A clinical prediction model to estimate the metastatic potential of pheochromocytoma/paraganglioma: ASES score. *Surgery.* 2018;164:511–7.
 31. Eisenhofer G, Tischler AS. Neuroendocrine cancer. Closing the GAPP on predicting metastases. *Nat Rev Endocrinol.* 2014;10:315–6.
 32. Eisenhofer G, Lenders JW, Timmers H, Mannelli M, Grebe SK, Hofbauer LC, Bornstein SR, Tiebel O, Adams K, Bratslavsky G, Linehan WM, Pacak K. Measurements of plasma methoxytyramine, normetanephrine, and metanephrine as discriminators of different hereditary forms of pheochromocytoma. *Clin Chem.* 2011;57:411–20.
 33. Eisenhofer G, Pacak K, Huynh TT, Qin N, Bratslavsky G, Linehan WM, Mannelli M, Friberg P, Grebe SK, Timmers HJ, Bornstein SR, Lenders JW. Catecholamine metabolomic and secretory phenotypes in phaeochromocytoma. *Endocr Relat Cancer.* 2010;18:97–111.
 34. Chiarugi P, Cirri P. Metabolic exchanges within tumor microenvironment. *Cancer Lett.* 2016;380:272–80.
 35. Kuroda N, Tamura M, Ohara M, Hirouchi T, Mizuno K, Miyazaki E, Hayashi Y, Lee GH. Possible identification of third stromal component in extraadrenal paraganglioma: myofibroblast in fibrous band and capsule. *Med Mol Morphol.* 2008;41:59–61.

36. D'Antongiovanni V, Martinelli S, Richter S, Canu L, Guasti D, Mello T, Romagnoli P, Pacak K, Eisenhofer G, Mannelli M, Rapizzi E. The microenvironment induces collective migration in SDHB-silenced mouse pheochromocytoma spheroids. *Endocr Relat Cancer*. 2017;24:555–64.
37. Richter S, D'Antongiovanni V, Martinelli S, Bechmann N, Rivero M, Poitz DM, Pacak K, Eisenhofer G, Mannelli M, Rapizzi E. Primary fibroblast co-culture stimulates growth and metabolism in Sdhb-impaired mouse pheochromocytoma MTT cells. *Cell Tissue Res*. 2018;374:473–85.
38. Blažević A, Hofland J, Hofland LJ, Feelders RA, de Herder WW. Small intestinal neuroendocrine tumours and fibrosis: an entangled conundrum. *Endocr Relat Cancer*. 2018;25:R115-30.
39. das Neves Pereira JC, da Silva AG, Soares F, Ab'Saber AM, Schmidt A, Rodrigues OR, Garippo A, Capelozzi M, de Campos JR, Takagaki T, Jatene FB, Martins S, Capelozzi VL. Nuclear and environment morphometric profile in tumor size and nodal metastasis of resected typical pulmonary carcinoid. *Pathol Res Pract*. 2004;200:459–67.
40. García-Suárez O, García B, Fernández-Vega I, Astudillo A, Quirós LM. Neuroendocrine tumors show altered expression of chondroitin sulfate, glypican 1, glypican 5, and syndecan 2 depending on their differentiation grade. *Front Oncol*. 2014;4:15. <https://doi.org/10.3389/fonc.2014.00015>.
41. Laskaratos FM, Rombouts K, Caplin M, Toumpanakis C, Thirlwell C, Mandair D. Neuroendocrine tumors and fibrosis: an unsolved mystery? *Cancer*. 2017;123:4770–90.

Publisher's note Springer Nature remains neutral with regard to jurisdictional claims in published maps and institutional affiliations.